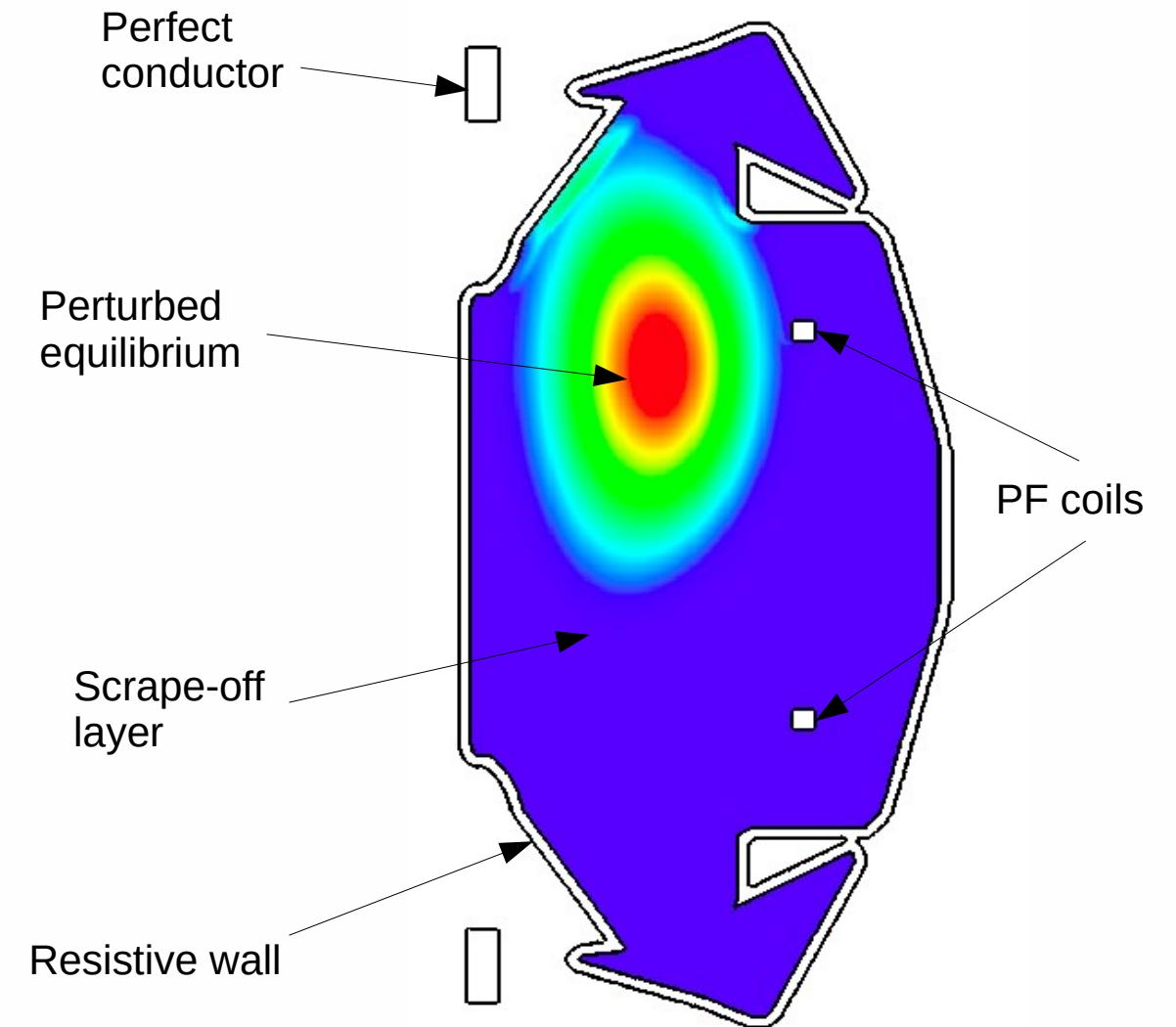


Numerical solutions of plasma flow in the presence of absolute vacuum

Maria Chrysanthou[†], S.T. Millmore, N. Nikiforakis
Laboratory for Scientific Computing, University of Cambridge

Outlook

- The objective of this work is to account for all regions of the reactor (plasma, scrape-off layer, wall) within the same simulation.
- Material boundary conditions are incorporated using state of the art sharp and/or diffuse interface methods.
- Hierarchical adaptive mesh refinement (AMReX framework) is used to resolve material boundaries and steep gradients.
- The end goal is the investigation of highly unstable events such as VDEs.
- In this presentation we focus on the representation of the scrape-off layer.



Framework

- The ideal MHD equations are solved using a conservative finite volume approach.

$$\begin{aligned}\frac{\partial \rho}{\partial t} + \nabla \cdot (\rho \mathbf{v}) &= 0, \\ \frac{\partial \rho \mathbf{v}}{\partial t} + \nabla \cdot \left[\rho \mathbf{v} \otimes \mathbf{v} + \left(p + \frac{1}{2} B^2 \right) \mathbf{I} - \mathbf{B} \otimes \mathbf{B} \right] &= 0, \\ \frac{\partial U}{\partial t} + \nabla \cdot \left[\left(U + p + \frac{1}{2} B^2 \right) \mathbf{v} - (\mathbf{v} \cdot \mathbf{B}) \mathbf{B} \right] &= 0, \\ \frac{\partial \mathbf{B}}{\partial t} + \nabla \cdot (\mathbf{B} \otimes \mathbf{v} - \mathbf{v} \otimes \mathbf{B}) &= 0.\end{aligned}$$

- Exact and/or approximate Riemann solvers, such as HLLC, are used to compute fluxes.
- Fluid-vacuum interfaces are fitted using a flux modified approach.

The Riemann problem

- A Riemann problem is defined as an initial value problem made up of a single discontinuity.
- For the MHD equations the solution to a RP consists of seven waves, which can either be discontinuities or rarefaction fans.
- Any hyperbolic system can be solved by computing the solution to a series of local RP at each cell interface.

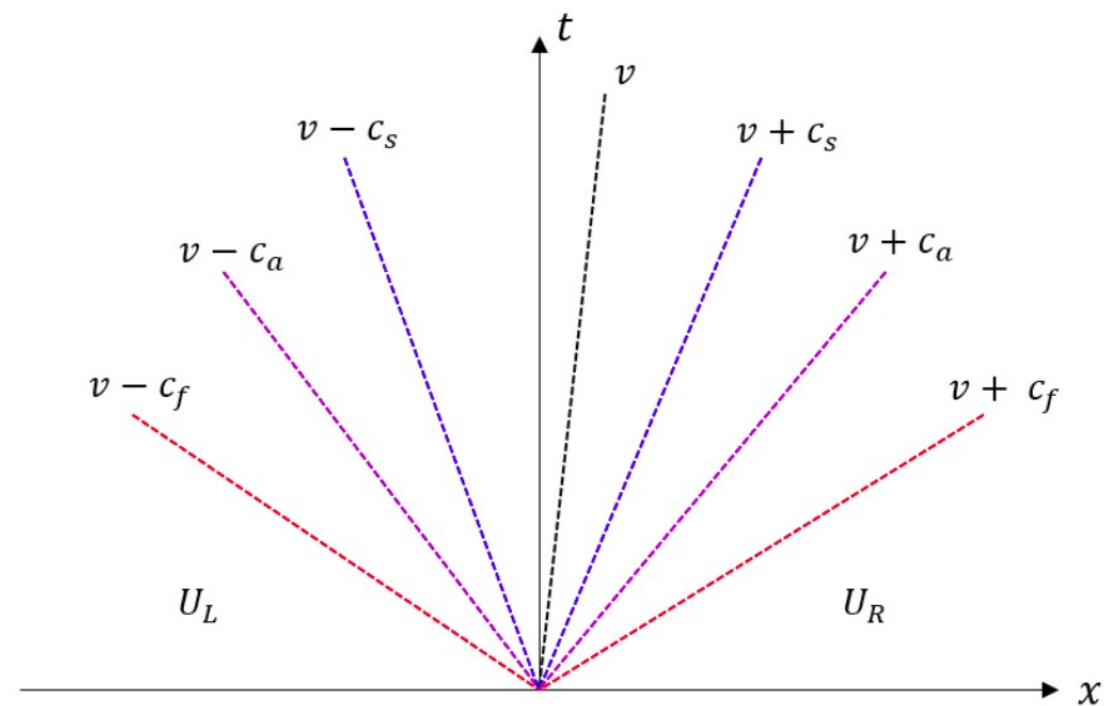


Figure: The characteristic wave pattern for a one-dimensional ideal MHD system, consisting of seven waves.

Exact Riemann solver for MHD

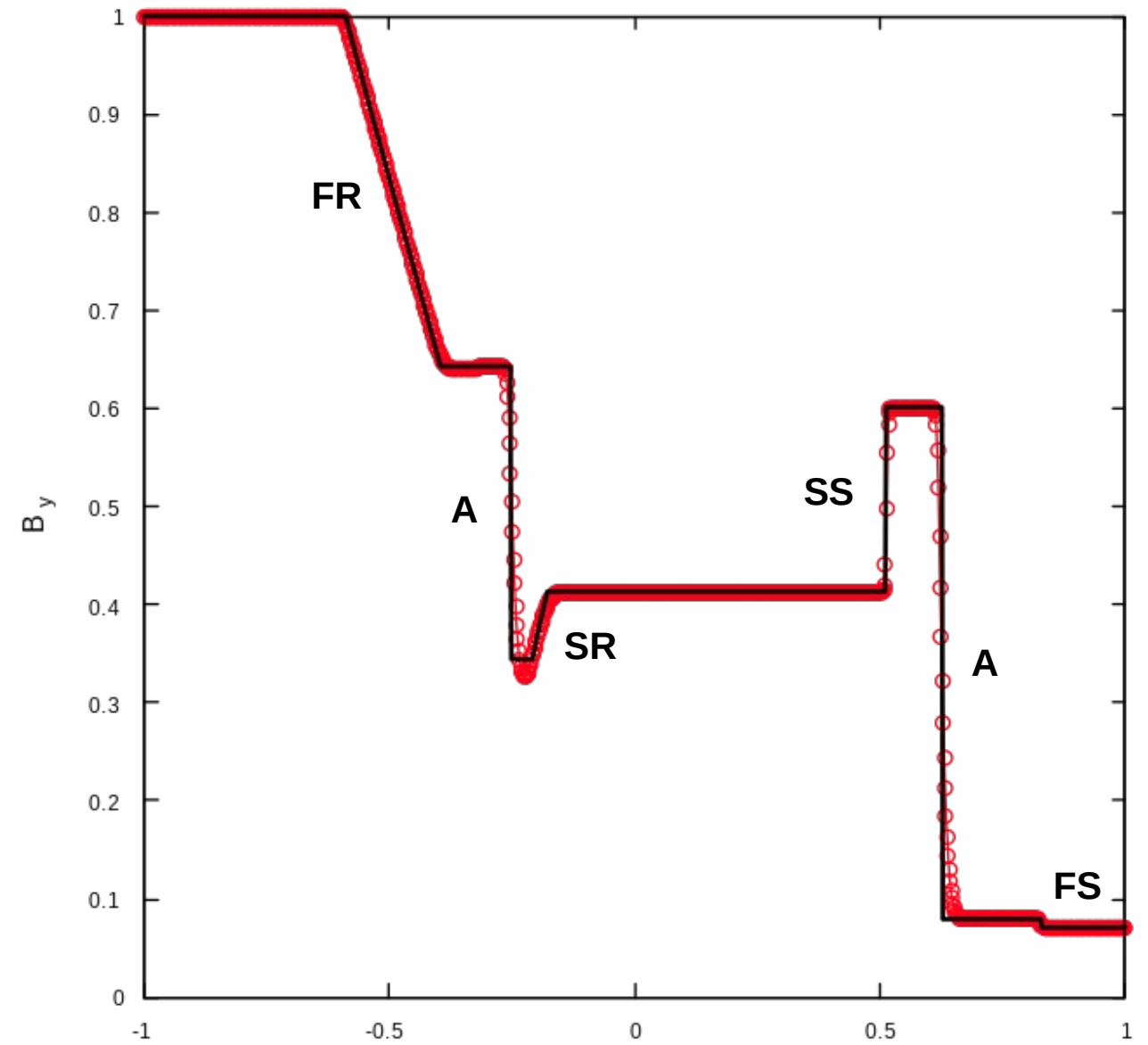
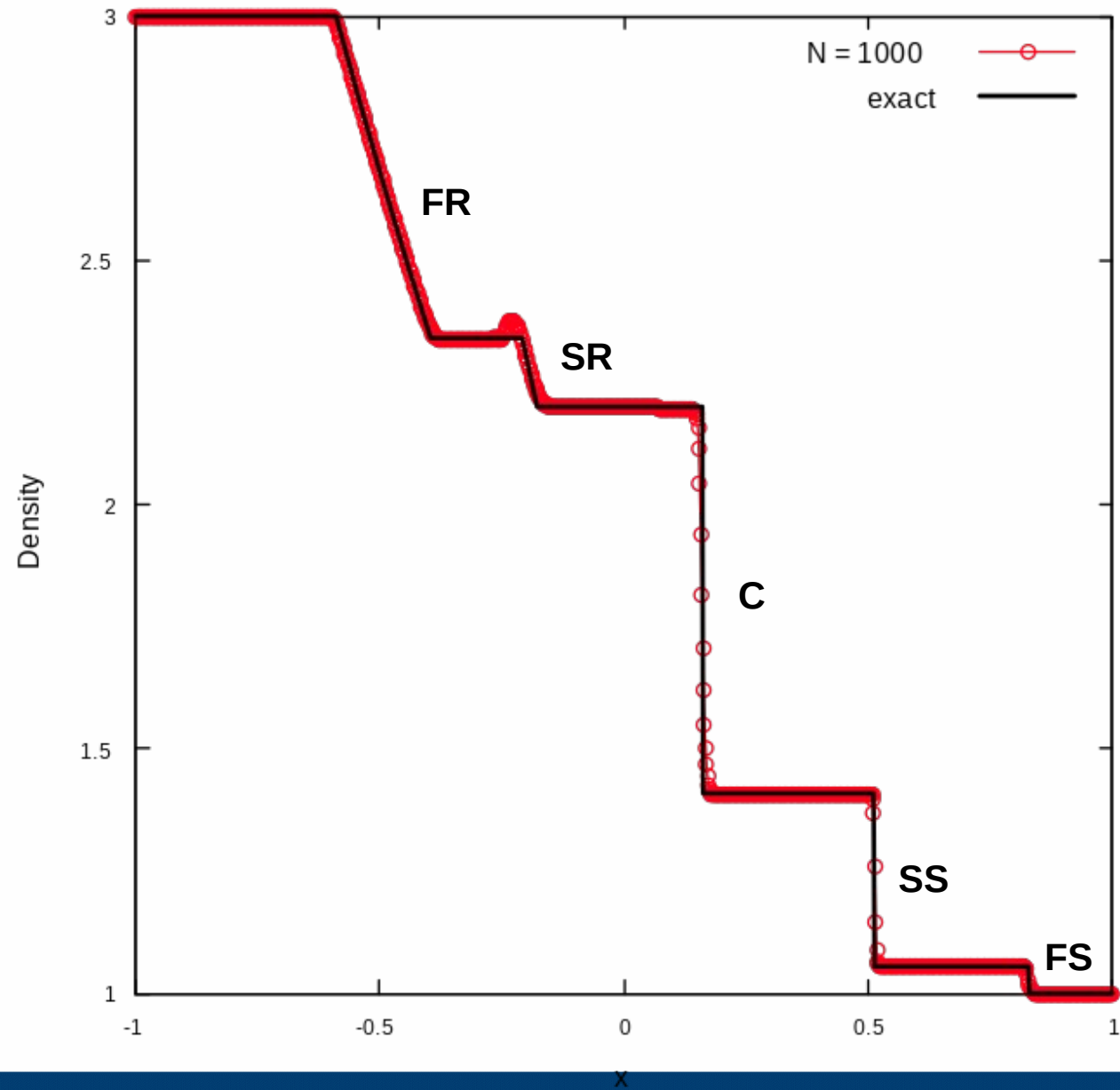
- The solution to a one-dimensional ideal MHD Riemann problem can admit up to seven waves.
- Each wave is mapped onto a path variable, resulting in a nonlinear system of equations.
- The equations can be reduced into a 5×5 system of the form

$$\text{RP}_U(\Psi) = \text{RP}_{U_0}^*(\psi_{s,f}^-, \alpha_{R0}) - \text{RP}_{U_1}^*(\psi_{s,f}^+, \alpha_T - \alpha_{R0}) = \mathbf{0} \in \mathfrak{R}^5,$$

where RP_U represents the Riemann problem for initial conditions $U = (U_0, U_1)$ and Ψ is the vector of path variables $(\psi_{s,f}^+, \alpha_{R0})$.

- This is solved using a multidimensional Newton-Raphson procedure in conjunction with Broyden's method.

Exact and numerical solutions for MHD RP



	ρ	v_x	v_y	v_z	p	B_x	B_y	B_z
Left	3.0	0.0	0.0	0.0	3.0	1.5	1.0	0.0
Right	1.0	0.0	0.0	0.0	1.0	1.5	$\cos(1.5)$	$\sin(1.5)$

Fluid – vacuum Riemann problem

- The fluid-vacuum RP is a special case RP, which poses important numerical challenges, due to the presence of a strong rarefaction and the disparity between the very small densities around the fluid-vacuum interface and the very large velocity of the vacuum front.

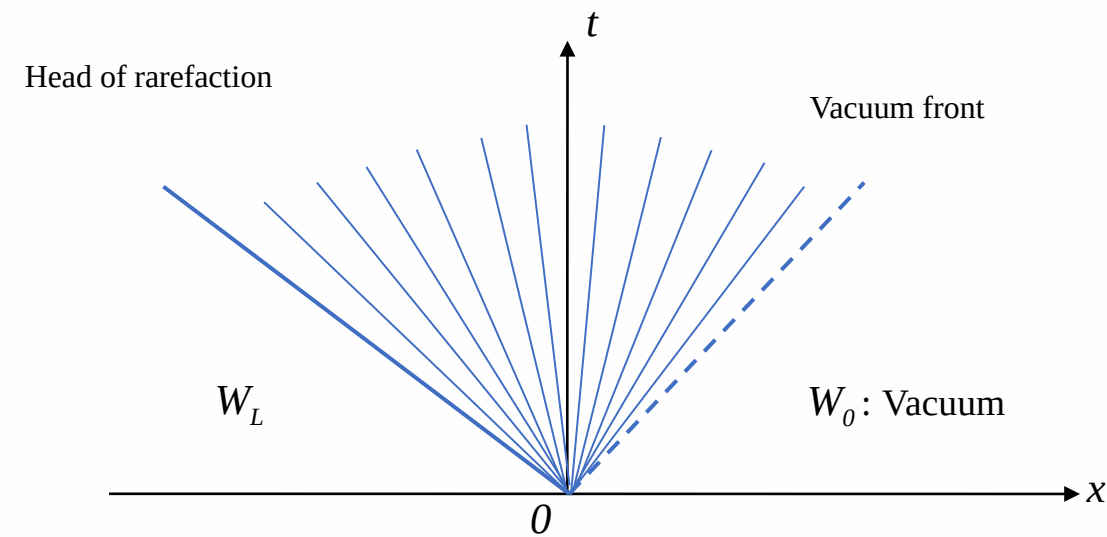


Figure: Riemann problem solution for a right vacuum state.

- Therefore, a major development of this work is the modification of the system of equations to enable realistic and physically consistent simulations of vacuum in the presence of magnetic fields.
- The first step is to consider the exact solution for the vacuum RP in the presence of magnetic fields.

Plasma-vacuum RP for varying magnetic field strengths

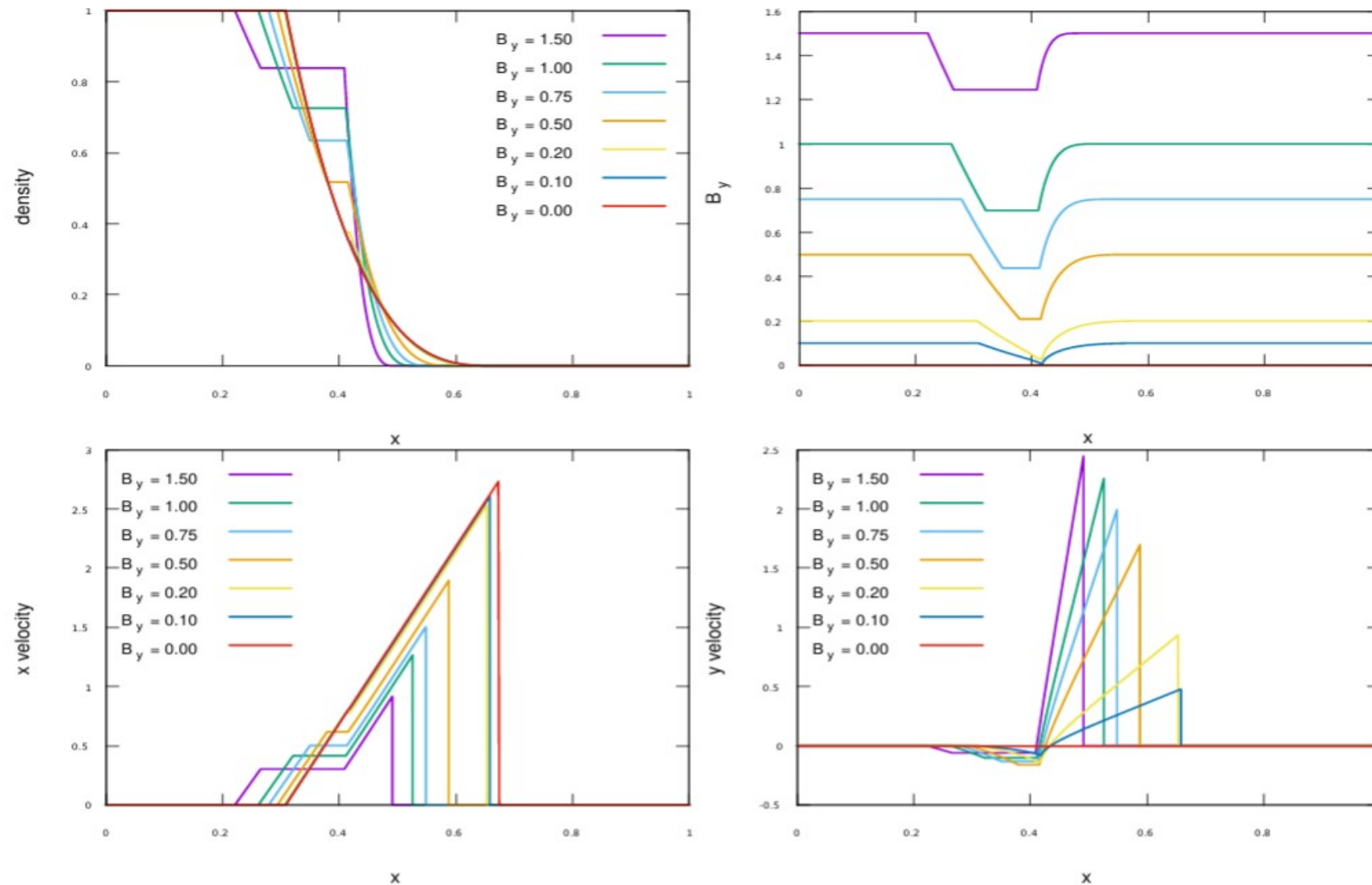


Figure: Exact solutions for plasma-vacuum Riemann problem, consisting of a fast rarefaction, a slow rarefaction and a contact wave at the plasma-vacuum interface.

	ρ	v_x	v_y	v_z	p	B_x	B_y	B_z
Left	1.0	0.0	0.0	0.0	0.5	0.375	(0.0, 0.1, 0.2, 0.5, 0.75, 1.0, 1.5)	0.0
Right	0.0	0.0	0.0	0.0	0.0	0.375	(0.0, 0.1, 0.2, 0.5, 0.75, 1.0, 1.5)	0.0

Fitting the plasma-vacuum interface

- We implement a novel diffuse interface method by Wallis *et al.* [2021] based on [flux modifiers](#) and [interface seeding routines](#).
- This requires the introduction of a new evolution equation for the void volume fraction variable.

$$\frac{\partial v}{\partial t} + \nabla \cdot v\mathbf{v} = v\nabla \cdot \mathbf{v}$$

- The entire system of equations is solved using a conservative monotone finite volume method which can accurately capture discontinuous solutions (HLLC solver with MUSCL reconstruction on primitive variables, RK3 in time.)
- MUSCL-BVD-THINC reconstruction is also implemented for minimising numerical diffusion around the interface.

Numerical method

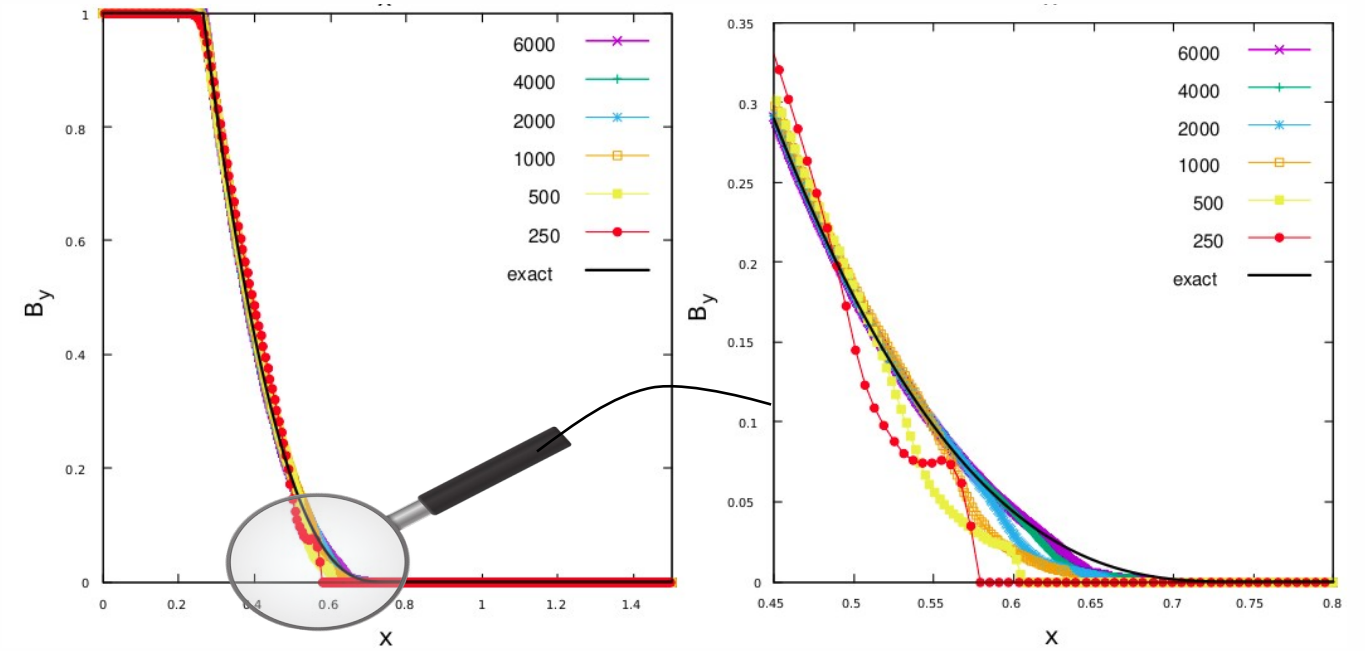
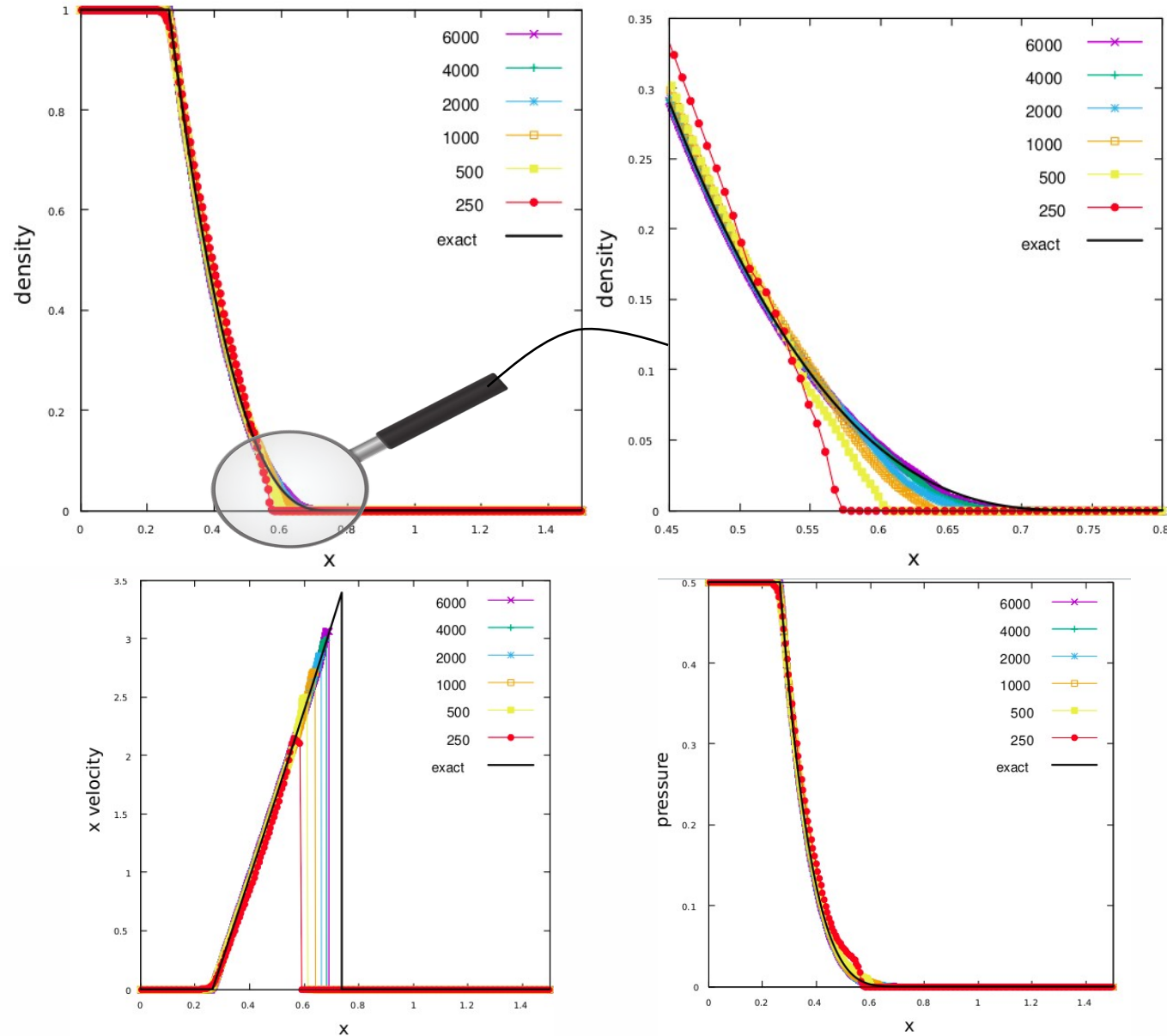
- Void seeding routine:
 1. In cells where $\nu \geq 0.9$, the void normal is calculated using Young's/ELVIRA method.
 2. A probe is sent along the normal and a new state \mathbf{U}_{interp} is interpolated.
 3. If $\nu_{interp} < \nu$, a new state is defined, so that $\mathbf{U}_{new} = \mathbf{U}_{interp}$.
 4. The new state is linearly combined with the original state, $\mathbf{U} \leftarrow (1 - \nu)\mathbf{U} + \nu\mathbf{U}_{new}$, but keeping the magnetic field variables and the void volume fraction variable constant.
- Flux modifier (improvement based on Munz's work [1994]):
 1. Cells are separated into three different types, fluid-fluid interface, fluid-void interface and void-void interface cells.
 2. Normal HLLC flux is computed for fluid-fluid interface cells and a modified flux is computed for fluid-void interface cells given by:

$$\mathbf{F}_{fi} = \begin{cases} \mathbf{F}_{fluid}^{HLLC} & \text{if } S_l \geq 0, \\ \frac{(S_r \mathbf{F}_{fluid}^{HLLC} - S_r S_l \mathbf{U}_{fluid})}{S_r - S_l} & \text{if } S_l < 0, \end{cases}$$

where $S_l = v_n^{fluid} - c_f^{fluid}$ and $S_r = v_n^{fluid} + \frac{2c_f^{gas}}{\gamma - 1}$.

fi : fluid-vacuum interface

Free expansion test case



	ρ	v_x	v_y	v_z	p	B_x	B_y	B_z
Test 2 Left	1.0	0.0	0.0	0.0	0.5	0.0	1.0	0.0
Test 2 Right	0.0	0.0	0.0	0.0	0.0	0.0	0.0	0.0

Free expansion vs low-density approximation

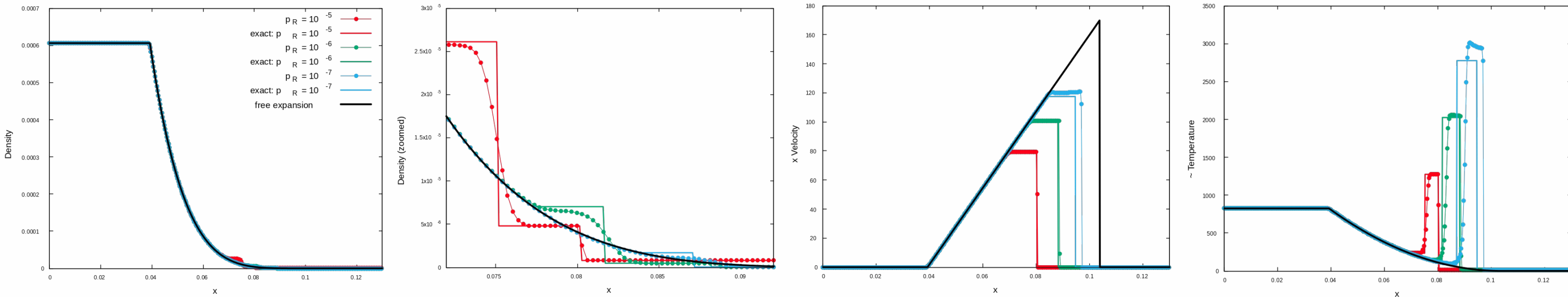
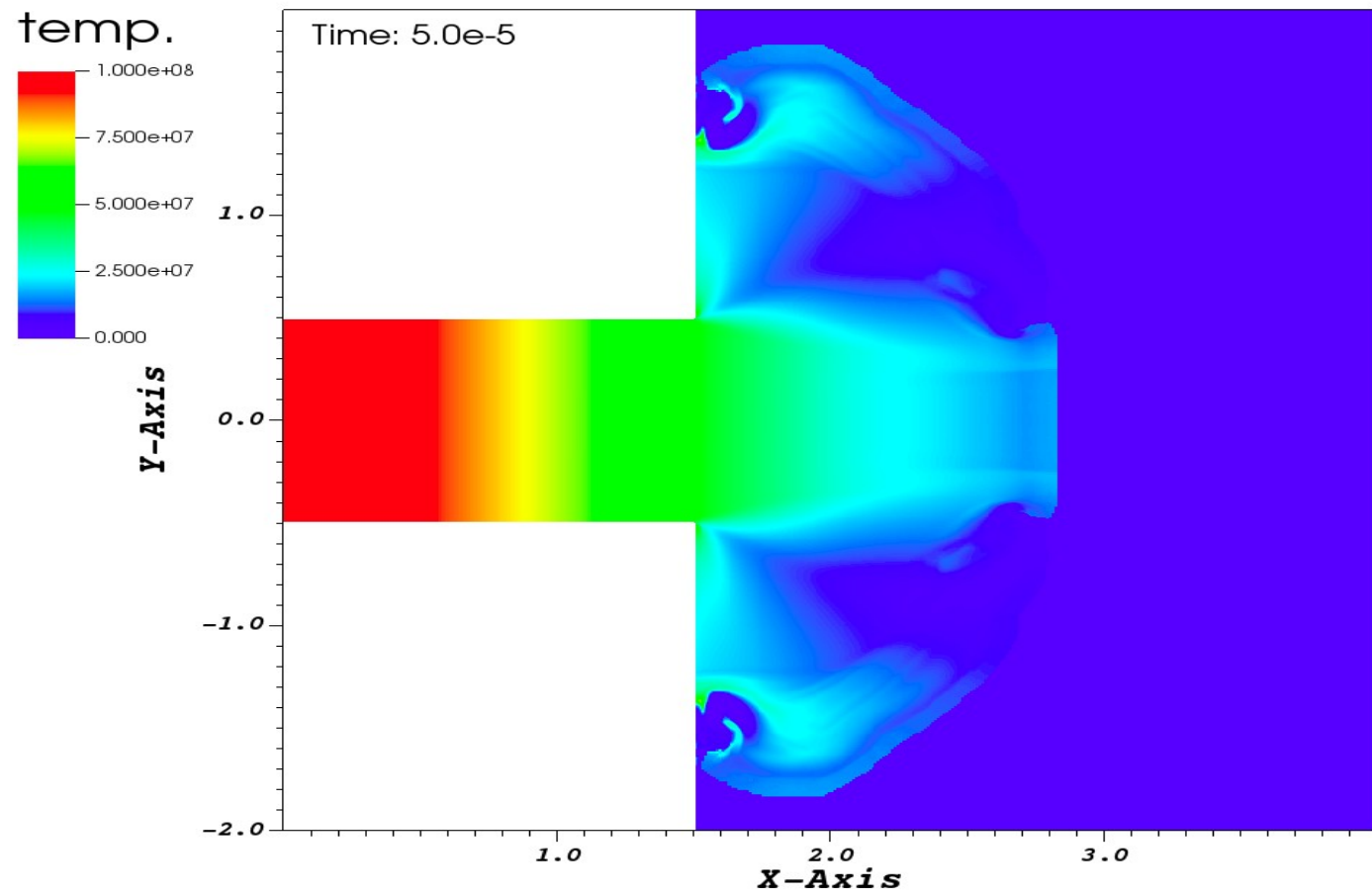


Figure: Exact solution for free expansion plotted against various low-density approximations. An **additional shock** is observed in the presence of a finite density in the background state.

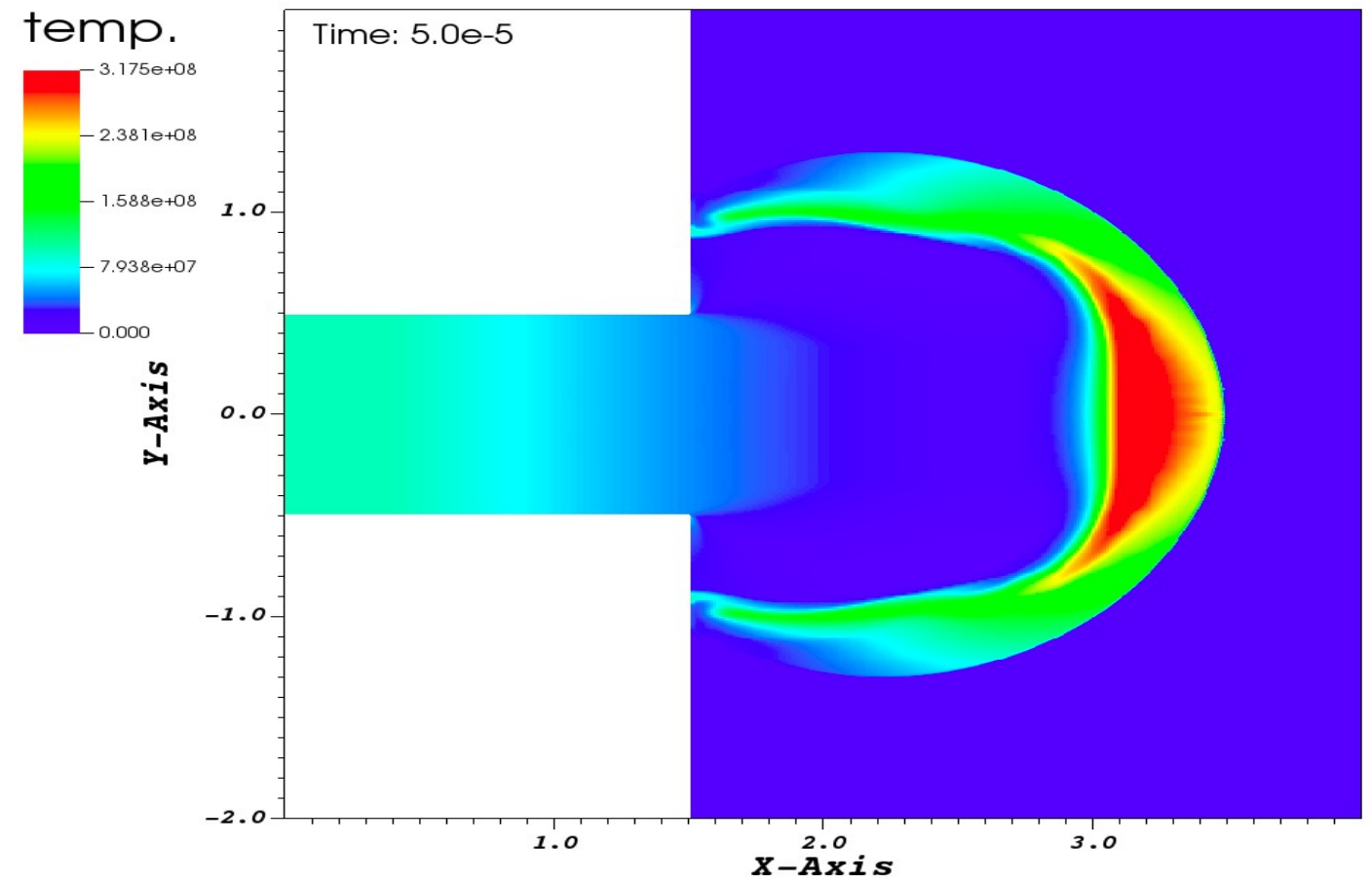
	ρ	p
Driver state	6.06×10^{-4}	0.5
Background state 1	8.08×10^{-7}	1×10^{-5}
Background state 2	8.08×10^{-8}	1×10^{-6}
Background state 3	8.08×10^{-9}	1×10^{-7}

Plasma accelerator test case

TRUE VACUUM SIMULATION

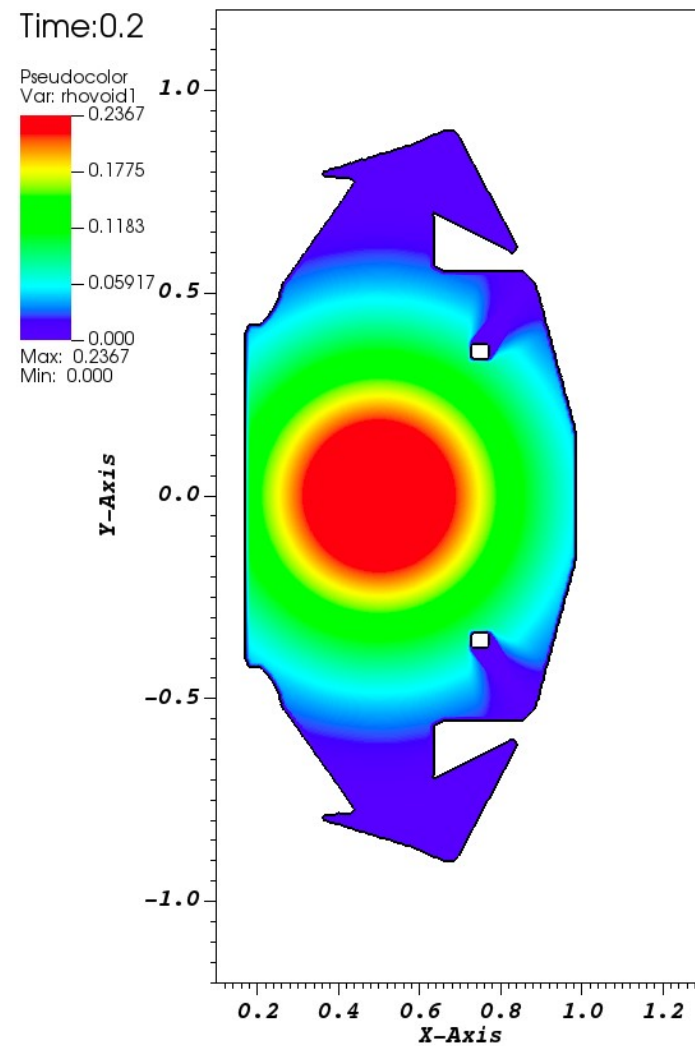


LOW DENSITY SIMULATION

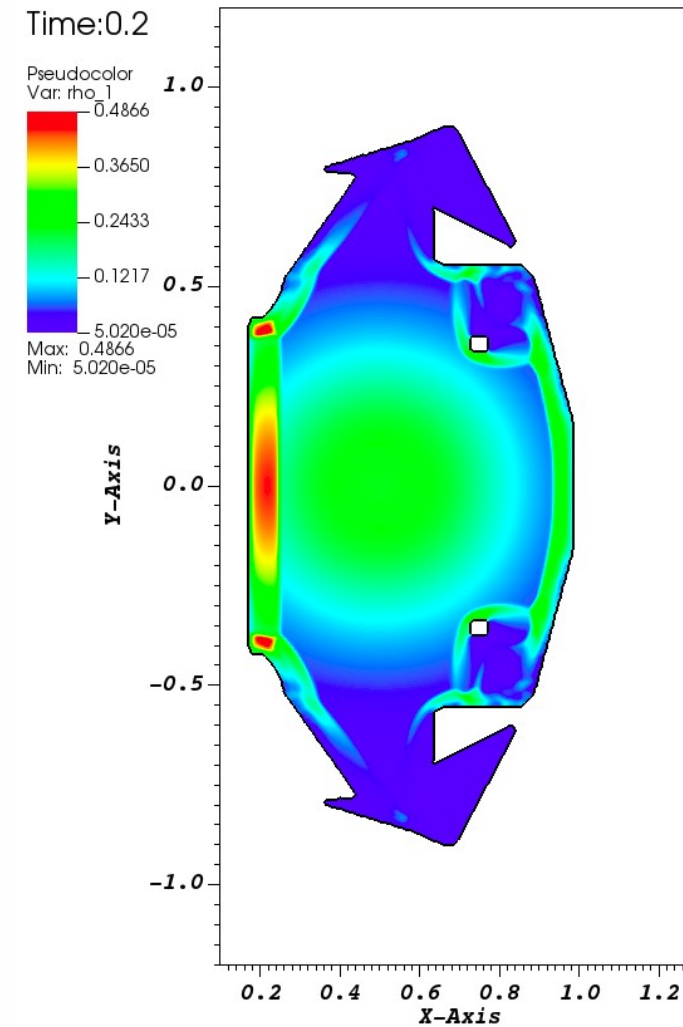


Plasma expansion in low density and vacuum background state within ST40 geometry

TRUE VACUUM SIMULATION



LOW DENSITY SIMULATION



Concluding remarks

- Considering alternative methodologies for the accurate and physical representation of the SOL.
- Demonstrated that low density approximations produce solutions that are physically inconsistent with the theory of free expansion.
- True vacuum solutions and low density approximation solutions result in distinct wave patterns which interact differently in the presence of a true material boundary.

- Addition of more physics (full model) :
 - Multi-species system
 - Kinetic closure relations
 - Elastoplastic reactor wall model (for computing heat loads on divertor)
- Enforcement of current free condition in vacuum region.
- Consideration and validation of unstable events within fusion reactors (e.g. ELMs and VDEs).